SEMARAK ILMU PUBLISHING

Journal of Advanced Research in Fluid Mechanics and Thermal Sciences

Journal homepage:
https://semarakilmu.com.my/journals/index.php/fluid_mechanics_thermal_sciences/index
ISSN: 2289-7879

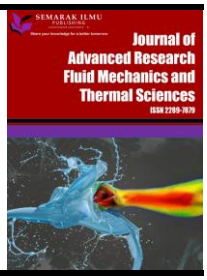

Numerical Solution of Darcy-Forchheimer Casson Nanofluid Flows with Joule Heating and Radiation

Tankashala Rajeshwai[1], Ramesh Kune[2,*], Hari Singh Naik Sabawat[3]

[1] Department of Mathematics, NTR Govt. Degree College for Women, Mahbubnagar, Telangana 509001, India
[2] Department of Science and Humanities, Sreenidhi Institute of Science and Technology, Yamnampet, Ghatkesar, Hyderabad, Telangana 501301, India
[3] Department of Mathematics, Osmania University, Hyderabad-500007, Telangana, India

ARTICLE INFO

Article history:
Received 5 October 2023
Received in revised form 2 January 2024
Accepted 16 January 2024
Available online 15 February 2024

Keywords:
Casson fluid; MHD; boundary layer flow; joule heat and radiation and joule heat; Darcy-Forchheimer; parameter

ABSTRACT

The present article provides a description of the hydrothermal properties of a Non – Newtonian nanofluid flow over a Darcy surface that is undergoing extension. The Darcy-Forchheimer effect is a phenomenon that describes the movement of nanofluids through a variable surface. The present study aims to investigate the impact of thermal radiation on heat transfer in magnetohydrodynamic (MHD) flow, utilizing a Casson nanofluid. The impacts of chemical reaction, magnetic field and thermal radiation are taken into consideration. The flow equations are transformed to ordinary differential equations by the appropriate similarity transformations. The Keller-Box method is used to compute the governing differential equations. It is found that the angle of inclination parameter enhances the thermal boundary layer thickness of the flow and the Joule heating parameter improves the thermal boundary layer thickness and slows the fluid velocity, which helps to maintain system temperature. The rate of Heat is increasing while mass transfer rate decreasing with the increasing values Brownian motion. Numerical and graphical results of various flow parameters as well as heat and mass rates are also provided in tables and graphs. So, the observation of the results systems for electronic devices, where the interaction of fluid flow, heat transfer, and electromagnetic effects is significant.

1. Introduction

In current periods, scientists are focusing on Nano fluids due to their vibrant warm air performance and remarkable effectiveness in heat transmission without any pressure drops. Nanofluid contains different types of particles, such as TiO_2, Al_2O_3 and Cu with oil, water and EG as a base fluid. It is discovered that the thermal conductivity of the base fluid and the Nano fluid differs. Choi and Eastman [1] took effort to create the term "nanofluid" and explain how thermal properties developed by mixing nanoparticles with base fluids. Williamson non-Newtonian fluid, in contrast to other nanofluids, has nil viscosity at rest and infinite viscosity as the shear rate approaches infinity.

* *Corresponding author.*
E-mail address: rameshkune@sreenidhi.edu.in

https://doi.org/10.37934/arfmts.114.1.7692

Buongiorno [2] investigated the reasons for the development of thermal conductivity of the Nano Fluid. He observed that the Nano fluid's thermal conductivity is enhanced by the Brownian motion. Elbashbeshy and Asker [3] explained the surface cooling effect is enhanced and thus nanofluids are appropriate as heat transfer nanofluid containing gyrotactic microorganisms over a vertical stretching surface embedded in a porous medium. The effect thermophoresis and Brownian motion on nanofluid study flow on stretching of a horizontal plate is observed by Tawade *et al.,* [4]. Explained buoyancy and solutal buoyancy parameter strongly influenced the nanofluid system by Nath and Murugesan [5]. The impact of suction and heat generation parameters on different types of nanoparticles such as copper and aluminum with base as water was discussed by Ahmad *et al.,* [6]. Ziaei-Rad *et al.,* [7] tested the pressure drop and heat transfer effects on in a mixed convection Nano fluid on permeable plate. Thumma *et al.,* [8] described the effects of the heat source and buoyancy parameters on radiative MHD Newtonian Nano fluid on oscillating variable permeable plate on a slanting surface. Selva Rani and Govindarajan [9] investigated the convective heat transfer of a different types of nanofluids over a variable sheet with changeable temperature. Illustrated the double diffusion of heat and mass transfer of Jeffery Nano fluid over a stretching plate by Khan *et al.,* [10]. Sarkar and Kundu [11] examined theoretically the coexistence of solar radiation and a Darcy-Forchheimer permeable medium is used to create a natural convection flow of an Ag nanoparticle-based nanofluid along an inclined flat sheet. Numerous researchers have recently looked at nanofluid, a few of them are taken from Bhatti *et al.,* [12].

So many researchers are showing interest in studying boundary layer flow and exchange of heat on variable sheets due to its significance in various fields, such as engineering for designing copper wires, elastic sheets, food processing and paper etc. Sakiadis [13] investigated boundary flow over a solid boundary layer and based on this steady can extend the boundary layer flow over movable surface and cylindrical surface. Konwar *et al.,* [14] examined the mixed convection MHD boundary layer flow, heat and mass transfer of a Newtonian fluid mixture across an exponentially stretched permeable sheet in porous medium with Soret and Dufour effects subject to temperature-dependent fluid properties. Ali *et al.,* [15] investigated the effect of various parameter on steady electromagnetic flow generated by stretching sheet. Ramesh *et al.,* [16] Examined the velocity and heat transfer in dusty flow over a linear stretching sheet with non-uniform heat souse/sink. Malik and Rehman [17] talked about the fluid flow resulting from natural convection across a vertical sheet. Ramesh *et al.,* [18] tested the mathematical modeling of convective boundary layer flow over an inclined movable flat plate. Griffiths [19] studied the boundary-layer flow across an inclined flat plate using non-Newtonian inelastic theory, indicated that the boundary-layer flow will be stabilized by the impact of shear-thinning. Pal and Mondal [20] investigated the effect of Thermophoresis and DuFour effects on a stretchable sheet over a changeable sheet. Pandya and Shukla [21] investigated the impact of Radiation on Incompressible MHD flow over on movable stretching sheet with viscous dissipations.

Due to the advancements in the technology and the extensive variety of applications in the process of investigation the non-Newtonian fluid which needs linear motion has curiosity attention. Nonlinear components are significant in the range of industries, including medicine and petrochemical manufacturing. The thickness of liquids varies depending on the distortion rate and certain liquids in nature possess an elastic element, which makes them to behave as non-fluids. Casson fluid has non-Newtonian rheological properties due to its shear stress and strain relationship. This fluid has a high shear viscosity and yields stress, making it an excellent indication for shear-thinning applications. Bhatti *et al.,* [22] analyzed the blood flow of the Casson fluid model with effect of entropy generation. Yanala *et al.,* [23] numerical solution of Casson fluid through a vertical plate was investigated. Shamshuddin *et al.,* [24] analyzed the thermal radiation effects on MHD Casson

fluid over an inclined porous plate. Many authors have investigated the flow of the Casson fluid model are choose from Prasad *et al.,* [25], and Jain and Parmar [26].

Ohmic heating is another name for joule heating. A conductor generates heat when an electric current flows through it, which raises the material's temperature. Due to this, it can use many electrical appliances, such as ovens, water warmers, and room heaters. Babu and Narayana [27] discussed Jeffrey fluid MHD mixed convection with the joule effect over a stretching sheet. Joule heating effect on the investigation of the non-Newtonian boundary layer flow across a vertical stretched sheet by Rao *et al.,* [28] Due to its many applications in real life, researchers focus curiosity on this study [29,30]. The Darcy-Forchhimier flow of the Nano fluid above a stretchable sheet is tested by Ganesh *et al.,* [31]. Haider *et al.,* [32] examined Darcy - Forchhimer flow over a rotation disk. The present work aims to improve the energy transference rate for industrial and biomedical applications.

Motivated by the above research work the present work seek to be analyze the heat and mass transform of MHD Darcy-Forchheimer equation of Casson Nanofluid through a stretching sheet with Joule heating, Heat source and Chemical reaction. No such work was done in the previous. There have been many studies looking into how different fluid characteristics affect Nano fluid flow. The modelled system of governing partial differential equations and associated boundary conditions to a system of ordinary differential equations with suitable transformation, ordinary differential equations corresponding to momentum, energy and concentration equations are derived. These equations are solved with the help of Keller Box technique. The effects of different flow parameters on velocity, temperature and concentration profiles are investigated and analyzed with the help of graphical representation.

2. Methodology

Consider the Casson Nanofluid boundary flow in two dimensions on a non-linear surface with the angle γ. The velocities are chosen $u_w(x) = ax^m$ and $u_\infty(x) = 0$. Where the coordinate axis - x is assumed in the inclined surface direction and 'a' is constant. It is assumed that the transverse magnetic field which is perpendicular to the direction of the flow of the fluid. T_w and C_w are consider nano fluid temperature and concentration at the wall. C_∞ and T_∞ are treated as the ambient forms of nano fluid mass and temperature. They are consummate since y tends to immensity, as indicated in the Figure 1.

i. The following hypotheses underlie this investigation.
ii. The extending free stream velocities are taken as the velocities are chosen $u_w(x) = ax^m$ and $u_\infty(x) = 0$.
iii. An external transverse magnetic field is assumed normal to the flow path.
iv. The Brownian motion and thermophoresis effects are considered.
v. The field temperature T and Nano particle fraction C at the wall take the constant values T_w and C_w.
vi. While the ambient forms for the Nano fluid mass and temperature fraction C_∞ and T_∞ are accomplished as Y approaches to immensity.

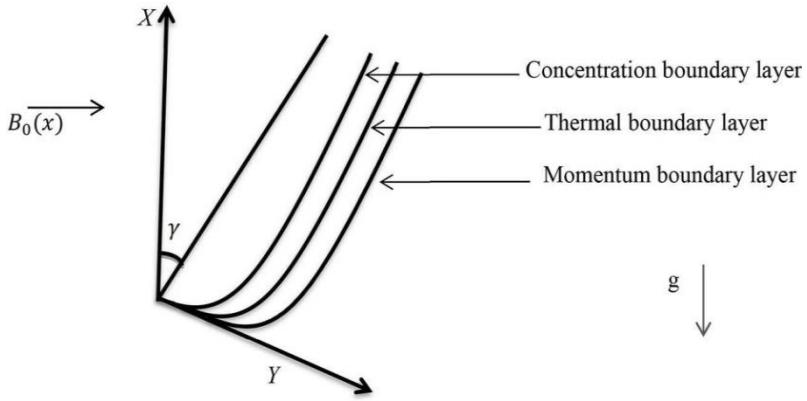

Fig. 1. Geometrical representation of flow model

The flow equations used in this research are provided by Rafique *et al.,* [33].

$$\frac{\partial u^*}{\partial x}+\frac{\partial v^*}{\partial y}=0 \tag{1}$$

$$u^*\frac{\partial u^*}{\partial x}+v^*\frac{\partial u^*}{\partial y}=\upsilon\left(1+\frac{1}{\beta}\right)\frac{\partial^2 u^*}{\partial y^2}+g\left[\beta_t^*\left(T^*-T^*_\infty\right)+\beta_c^*\left(C^*-C^*_\infty\right)\right]\cos\gamma-\frac{\sigma B_0^2\left(x\right)u^*}{\rho}-\frac{C_b}{\sqrt{K^*}}u^{*2} \tag{2}$$

$$u^*\frac{\partial T^*}{\partial x}+v^*\frac{\partial T^*}{\partial y}=\alpha\frac{\partial^2 T^*}{\partial y^2}-\frac{1}{\left(\delta c\right)_f}\frac{\partial q_r}{\partial y}+\tau\left[D_B\frac{\partial C^*}{\partial y}\frac{\partial T^*}{\partial y}+\frac{D_T}{T_\infty}\left(\frac{\partial T^*}{\partial y}\right)^2\right]+\frac{D_T K_T}{C_s C_p}\frac{\partial^2 C^*}{\partial y^2}+\frac{\sigma B_0^2}{\rho c_p}u^{*2} \tag{3}$$

$$u^*\frac{\partial C^*}{\partial x}+v^*\frac{\partial C^*}{\partial y}=D_B\frac{\partial^2 C^*}{\partial y^2}+\frac{D_T K_T}{T_\infty}\frac{\partial^2 T^*}{\partial y^2}-K_0\left(C^*-C^*_\infty\right) \tag{4}$$

By the help of Taylor series T^4 around T_∞ and ignoring higher order terms for:

$$T^{\square 4}\cong 4T_\infty^{\square 3}T^{\square}-3T_\infty^{\square 4} \tag{5}$$

$$u^{\square}\frac{\partial T^{\square}}{\partial x}+v^{\square}\frac{\partial T^{\square}}{\partial y}=\left(\alpha+\frac{16\sigma^*}{3k^*\left(\delta c\right)_f}\right)\frac{\partial^2 T^{\square}}{\partial y^2}+\tau\left[D_B\frac{\partial C^{\square}}{\partial y}\frac{\partial T^{\square}}{\partial y}+\frac{D_T}{T_\infty^{\square}}\left(\frac{\partial T^{\square}}{\partial y}\right)^2\right]+\frac{D_T K_T}{C_s C_p}\frac{\partial^2 C^{\square}}{\partial y^2}+\frac{\mu}{\rho c_p}u^{\square 2} \tag{6}$$

where u and v denotes the components of velocity in x and y directions. D_B represents the Brownian motion coefficient and the thermophoresis diffusion is indicated by D_T, coefficient k represents thermal conductivity, $\alpha=\dfrac{k}{\left(\delta c\right)_f}$ represents the parameter known as thermal diffusivity, and $\tau=\dfrac{\left(\delta c\right)_p}{\left(\delta c\right)_f}$ indicates the ratio of the base fluid's and nanoparticle's effective heat capacity.

The appropriate B.Cs are:

$$\begin{aligned} &At\ y=0,\ u^*=u_w\left(x\right)=ax^n,\ C^*=C_w^*,\ T^*=T_w,\ v=0,\\ &as\ y\to\infty,\ u^*\to u_\infty\left(x\right)=0,\ v^*\to 0,\ C^*\to C_\infty^*,\ T^*\to T_\infty^*, \end{aligned} \tag{7}$$

The stream function $\psi=\psi\left(x,y\right)$:

where $u^*=\frac{\partial\psi}{\partial y}, v^*=-\frac{\partial\psi}{\partial x}$. (8)

The following are the similar transformations.

$$\psi=\sqrt{\frac{2vax^{m+1}}{m+1}}f\left(\eta\right),\ \theta\left(\eta\right)=\frac{T^*-T_\infty^*}{T_w^*-T_\infty^*}, \phi\left(\eta\right)=\frac{C^*-C_\infty^*}{C_w^*-C_\infty^*}, \eta=y\sqrt{\frac{\left(m+1\right)ax^{m-1}}{2v}} \tag{9}$$

The equations in the system (3) to (7) can be summarized as non-linear ODEs by substituting (Eq. (8))

$$\left(1+\frac{1}{\beta}\right)f'''+ff''-\left(\frac{2m}{m+1}\right)f'^2+\frac{2}{m+1}\left(\lambda\theta-\theta\phi\right)\cos\gamma-\left(\frac{2M}{m+1}\right)f'-\frac{2m}{m+1}F_r\left(f'\right)^2=0 \tag{10}$$

$$\left(1+\frac{4}{3}R\right)\theta''+f\theta'+N_b\phi'\theta'+N_t\theta'^2+D_f\phi''+J\left(f'\right)^2=0 \tag{11}$$

$$\phi''+Lef\phi'+SrLe\theta''-LeK_r\phi=0 \tag{12}$$

where,

$$\begin{aligned} &\lambda=\frac{Gr_x}{\mathrm{Re}^2}, \delta=\frac{Gc}{\mathrm{Re}^2},\ M=\frac{\sigma B_0^2(x)}{a\rho(n+1)}, Ec=\frac{u_w^2}{\left(T_w-T_\infty\right)c_p}\ Le=\frac{\upsilon}{D_B}, \mathrm{Pr}=\frac{\upsilon}{\alpha},\ \ F_r=\frac{x}{(n+1)}\sqrt{\frac{1}{K^*}}C_b,\ \ J=Ec*M,\\ &Ec=\frac{\upsilon^2ax^{n+1}}{c_p(n+1)\left(T_w^*-T_\infty^*\right)}\ K_r=\frac{K_0}{\left(\frac{n+1}{2}\right)ax^{n-1}}, N_b=\frac{\tau D_B\left(C_w^*-C_\infty^*\right)}{\upsilon}, N_t=\frac{\tau D_B\left(T_w^*-T_\infty^*\right)}{\upsilon T_\infty},\ Gr_x=\frac{g\beta_t\left(T_w^*-T_\infty^*\right)x^3}{\upsilon^2},\\ &Gc_x=\frac{g\beta_c\left(C_w^*-C_\infty^*\right)x^3}{\upsilon^2},\ \mathrm{Re}=\frac{ax^{m+1}}{\upsilon},\ N=\frac{4\sigma^*T_\infty^3}{\alpha k^*}, D_f=\frac{D_TC_T\left(C_w^*-C_\infty^*\right)}{\upsilon C_sC_p\left(T_w^*-T_\infty^*\right)},\ Sr=\frac{D_TC_T\left(T_w^*-T_\infty^*\right)}{\upsilon T_\infty\left(C_w^*-C_\infty^*\right)}, \end{aligned} \tag{13}$$

In which the prime signifies the derivative corresponding to η, λ and δ thermal and Solutal Buoyancy parameter, F_r Forchheimer's parameter, M is known as the magnetic parameter, whereas Pr represents the Prandtl number, Le indicates Lewis number, N_b and N_t specifies the Brownian motion and the parameter which is called thermophoresis parameter, and radiation parameter is denoted by R.

The transformed B. Cs are transformed into:

$$f(\eta)=0,\ f'(\eta)=1,\ \theta(\eta)=\phi(\eta)=1\ at\ \eta=0,$$
$$f'(\eta)\to 0,\ \ \phi(\eta)\to 0,\theta(\eta)\to 0,\ as\ \eta\to\infty \tag{14}$$

For the current issue, the skin friction, Sherwood number, and Nusselt numbers are defined as follows

$$Nu_x=\frac{xq_w^*}{k\left(T_w^*-T_\infty^*\right)},\ Sh_x=\frac{xq_m^*}{D_B\left(C_w^*-C_\infty^*\right)},C_f=\frac{\tau_w^*}{u_w^2\rho_f} \tag{15}$$

$$q_w^*=-k\frac{\partial T^*}{\partial y},\ q_m^*=-D_B\frac{\partial C^*}{\partial y},\ \tau_w^*=\mu\left(1+\frac{1}{\beta}\right)\frac{\partial u^*}{\partial y}at\ \ y=0 \tag{16}$$

The non–dimensional skin friction coefficients C_{fx}, Sherwood number $-\phi'(0)$ and Nusselt number $-\theta'(0)$ are demarcated as

$$-\theta'(0)=\frac{Nu_x}{\left(1+\frac{4}{3}N\right)\sqrt{\frac{m+1}{2}\mathrm{Re}}},-\phi'(0)=\frac{Sh_x}{\sqrt{\frac{m+1}{2}\mathrm{Re}}},\ C_{fx}=C_f\sqrt{\frac{2}{m+1}\mathrm{Re}} \tag{17}$$

where, $\mathrm{Re}=\frac{u_w x}{\upsilon}$.

3. Procedure

Stage 1: In the early stage, all ODEs must be converted to first-order ODEs. (10) - (12).

$$f'=p,\ p'=q,\theta'=t,\phi'=g$$

$$\left(1+\frac{1}{\beta}\right)q'+fq-\left(\frac{2m}{m+1}+F_r\right)p^2+\frac{2}{m+1}(\lambda\theta-\theta\phi)\cos\gamma-\left(\frac{2M}{m+1}\right)p=0 \tag{18}$$

$$\frac{1}{\mathrm{Pr}}\left(1+\frac{4}{3}R\right)t'+ft+N_b gt+N_t t^2+D_f g+Jp^2=0 \tag{19}$$

$$g'+Lefg+SrLet'-K_r Le\phi=0 \tag{20}$$

$$f(\eta)=0,\ p(\eta)=1,\ \theta(\eta)=\phi(\eta)=1\ at\ \eta=0$$
$$p(\eta)\to 0,\ \theta(\eta)\to 0,\ \phi(\eta)\to 0\ \ as\ \eta\to\infty \tag{21}$$

3.1 Separation of Domains

Discretization is crucial in the subject of consciousness. Discretizing is often accomplished by dividing the space into equal-sized grids. In order to get a greater precision for the computation results, smaller grids are used.

$$\eta_0 = 0,\ \eta_j = \eta_{j-1} + h_j, \qquad j = 1,2,3.....,j-1,\ \eta_j = \eta_\infty, \qquad j = 1,2,3.....,J,\ \eta_j = \eta_\infty$$

Here $\left(h_j, k_j\right)\ n, j$ are equitable numbers in the sequence which indicates the position of the coordinates. For estimation of speed estimation, temperature and concentration changes make the initial assumption between $\eta = 0, \eta = \infty$. The frame works from the outcome have been presented as approximations of solutions. It is very difficult to find out the outcomes need to be equal using various preface estimates, but the reproduce calculations are varied by incorporating significant differences, differences and the use of functions to substitute the average values. Eq. (18) to Eq. (20) are converted into non-linear algebraic formulas.

3.2 Newton's Technique of Linearization

As a consequence of Newton's method. The (i+1)th iterations of the formulae possibly to be discovered in the preceding equations $(\ )_n^{(i+1)} = (\ )_n^{(i)} + \delta(\ )_n^{(i)}$ and once the higher-elevated boundaries have been ignored of $\delta(\ )_n^{(i)}$ an equation system with linear tri-diagonals.

3.3 The Bulk Scheme and Eliminating

The equation $F\delta = r$ has resulted in a bulk tri-diagonals matrix.

where

$$F.\delta = r$$

$$where, F = \begin{bmatrix} A_1 & C_1 & & & & & \\ B_2 & A_2 & C_2 & & & & \\ & \ddots & \ddots & \ddots & & & \\ & & & B_{j-1} & A_{j-1} & C_{j-1} & \\ & & & & B_j & C_j & \end{bmatrix}, \delta = \begin{bmatrix} \delta_1 \\ \delta_2 \\ \delta_3 \\ \vdots \\ \delta_{j-1} \\ \delta_j \end{bmatrix} and\ r = \begin{bmatrix} r_1 \\ r_2 \\ r_3 \\ \vdots \\ r_{j-1} \\ r_j \end{bmatrix} where\ F\ is\ 7 \times 7\ block-sized \qquad (22)$$

Matrix, it is equivalent to the size $j \times j$, $\delta\ and\ r\ are\ j \times 1$ ordered vectors. Now an efficient LU factorization process is applied to solve for δ. In $F.\delta = r$, where F=LU.

4. Results and Discussion

Once the system of ordinary differential equations is solved, different types of numerical answers are found. Then, these answers are shown and understood through graphs, which can be seen in figures.

Figure 3 and Figure 4 show how the magnetic field (M) affects the temperature and velocity curves. Increasing the parameter M creates Lorentz's force, and the strength of this force is directly related to the strength of the magnetic field. As M goes up, the Lorentz force goes up, which slows down the speed outline. We can see the opposite effect on temperature. Figure 5 shows that as the Pradallel number goes up, the thickness of the thermal boundary layer goes down and the temperature of the stream goes down. Figure 6 and Figure 7 show how Soret affects concentration, temperature and movement. Shows how a reduction in temperature and the corresponding thickness of the boundary layer are correlated with an increase in the Soret number. The reason for the decrease in temperature profile is really the decrease in thermal diffusion of the material caused by a rise in Soret number and same result in velocity curve, while the mass transfer accelerates as the values of Sr.

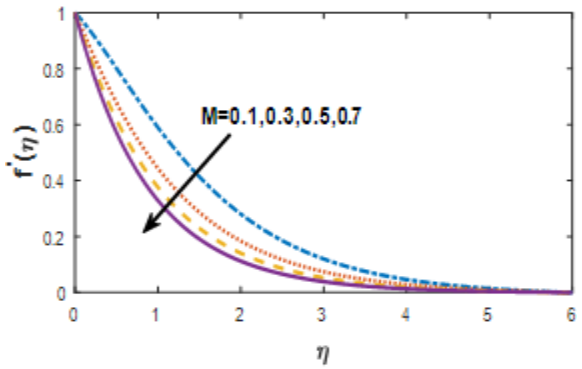

Fig. 3. M's effect on Velocity

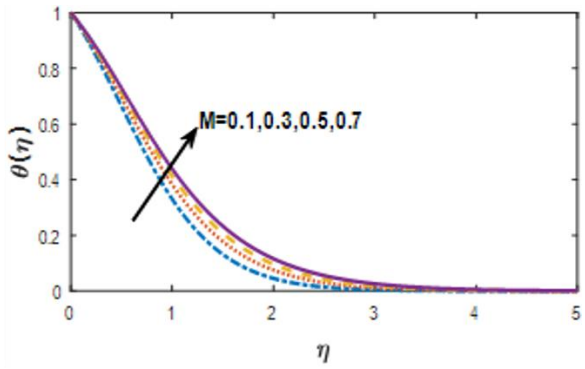

Fig. 4. M's effect on Temperature

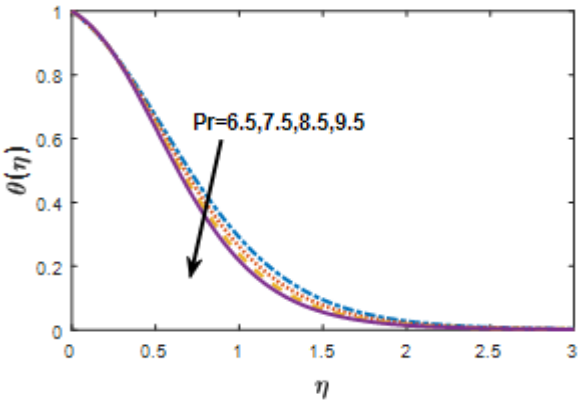

Fig. 5. Pr's effect on Temperature

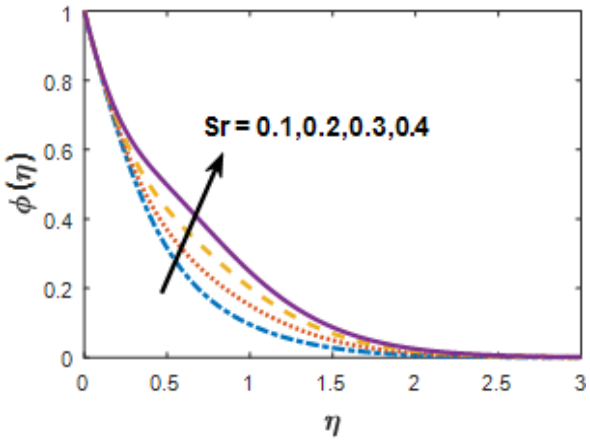

Fig. 6. Sr's effect on Concentration

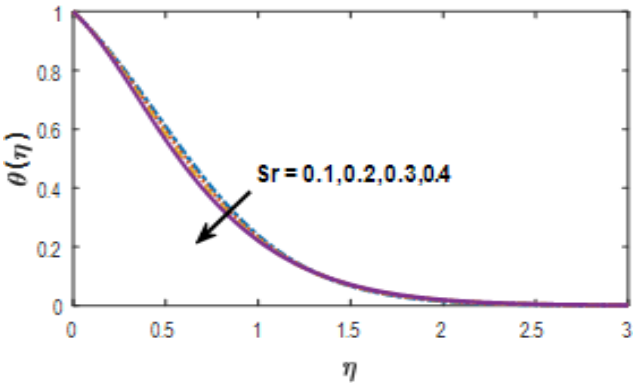

Fig. 7. Sr's effect on Temperature

Figure 8 and Figure 9 show that the effects of DuFour on concentration and temperature are demonstrated. Because the rate of energy transmission between particles increases when Dufour values climb, the temperature profiles improve as a result. Conversely, a rise in particle transmission concentration results in a drop in fluid concentration.

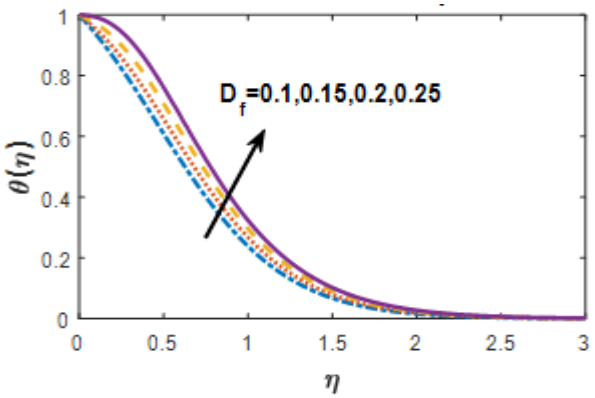

Fig. 8. D_f's effect on Temperature

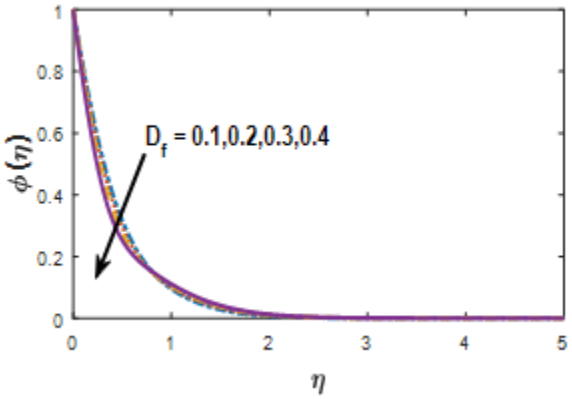

Fig. 9. D_f's effect on Concentration

In Figure 10, the temperature profile is shown to increase as R values rise. This is because a higher radiation parameter causes the fluid to heat up more, raising the temperature and thickening the thermal boundary layer. Figure 11 and Figure 12 demonstrate the stretching sheet (m) effects on velocity and temperature. It is noticed that increase in m, raises the velocity profile. It is because the stretching sheet affect raise the fluid flow strength, which increases the velocity and thickness of the boundary layer, reverse results observed in temperature field.

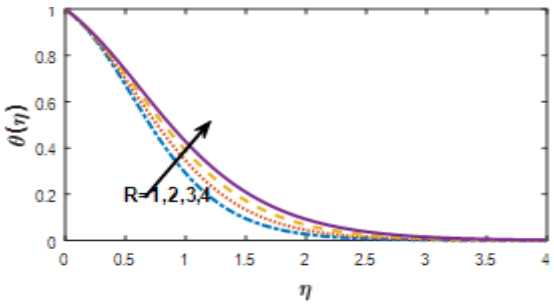

Fig. 10. Sr's effect on Temperature

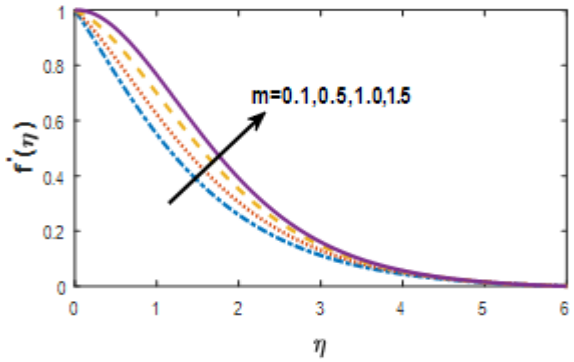

Fig. 11. m's effect on Velocity

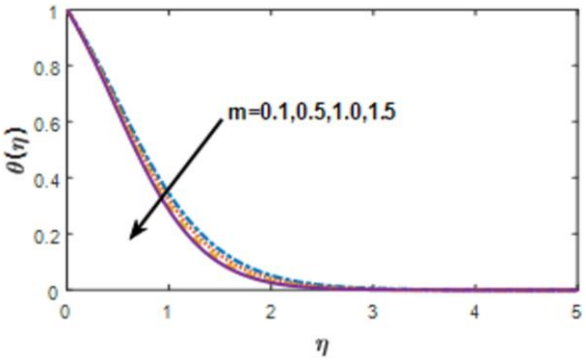

Fig. 12. m's effect on Temperature

Figure 13 illustrates the temperature diagram discrepancy for a variety of (Nb)Brownian motion parameters. In a physical sense, an increase in the Brownian motion parameter causes the nanofluid molecules to move significantly, leading to an increase in their kinetic energy and the production of more heat. As a direct consequence, there was an increase in the fluid's temperature. Figure 14 displayed the effects of thermophoresis parameter on temperature. It has been shown that as Nt increased, temperature profile is increased.

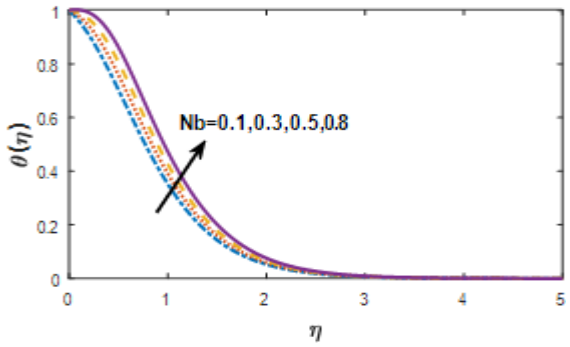

Fig. 13. Nb's effect on Temperature

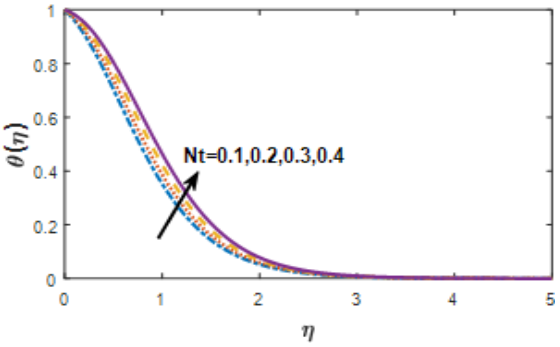

Fig. 14. Nb's effect on Temperature

Figure 15 explains the importance of the inclination angle factor Υ in the velocity. As increasing the value of Υ the velocity outline slow down. For the various values of the Le, the concentration profile is observed in graph Figure 16. The concentration is drops as up surge the values of Le.

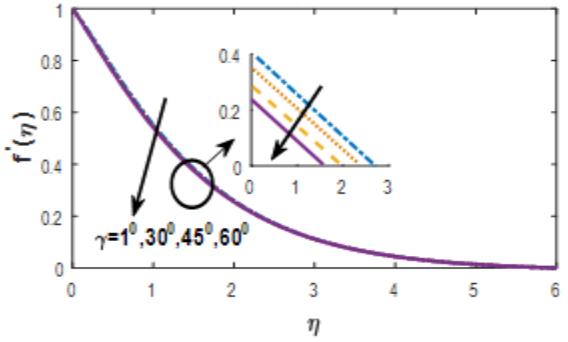

Fig. 15. γ's effect on Velocity

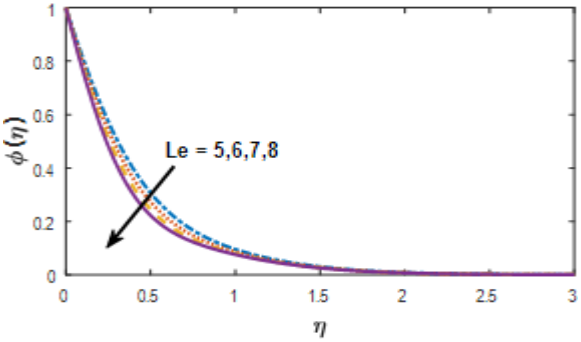

Fig. 16. Le's effect on Concentration

Figure 17 demonstrates how the concentration is affected by the chemical reaction parameter. As a component of a chemical process, increases the conversion rate of the fluid particle. This causes drops in fluid Concentration.

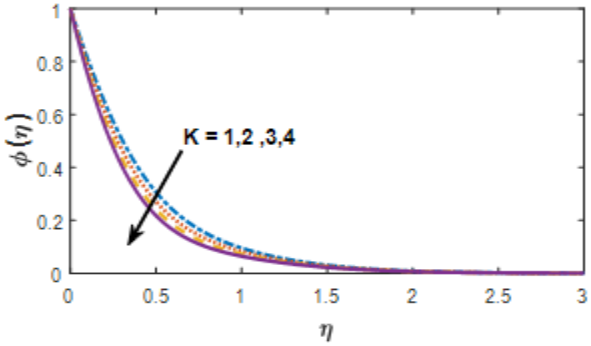

Fig. 17. K's effect on Concentration

Figure 18 shows the effect on the velocity with different values of Casson parameter β. As the Casson parameter (β) increases, the boundary layer thickness will be thinner, which leads to reduce the velocity of the flow.

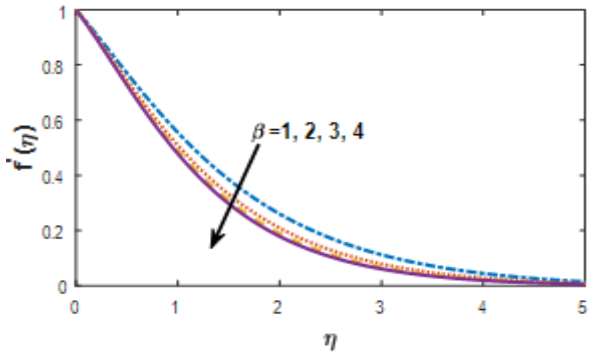

Fig. 18. β's effect on Velocity

The impact of the Forchheimer parameter (Fr) on the temperature profile and velocity may be observed in Figure 19 and Figure 20, respectively. It should be mentioned that increasing the value of Fr results in a decrease in fluid flow velocity. Figure 20 shows that when the Frochheimer parameter grows, so do the thermal gradients and the thickness of the related boundary layer. An increase in the Forchheimer parameter indicates the generation of resistive forces in the system. This causes the fluid's motion to diminish, which lowers the fluid's velocity. Furthermore, the drag force, which tilts the thermal gradients, raises the fluid's temperature. Figure 21 and Figure 22 describe the effects of the Joule heating parameter (J) on temperature and concentration profiles. The joule law states that the heat produced by an electric current is equal to the product of the resistance of the conductor, the square of the current and the lines in the flow with the conductor temperature at which joules of heat are produced. As the levels of the Joule parameters increase, the fluid temperature increases and the concentration profile reduce.

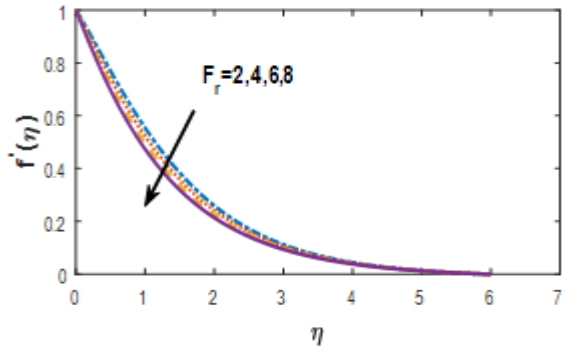

Fig. 19. F_r's effect on Velocity

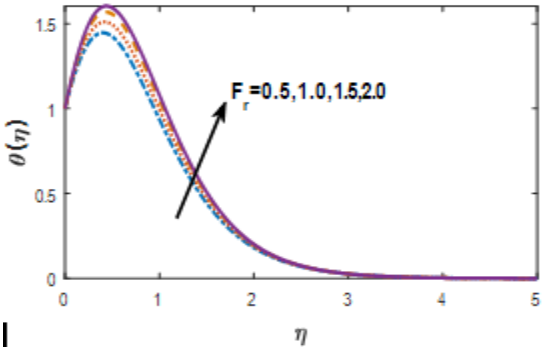

Fig. 20. F_r's effect on Temperature

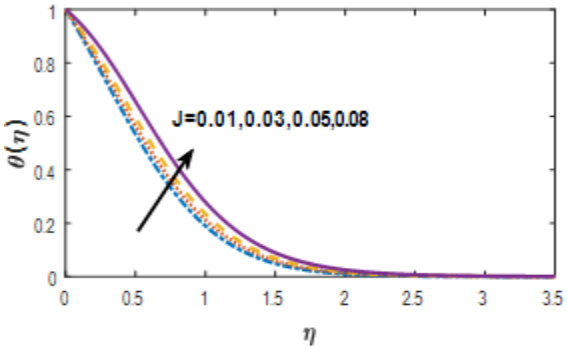

Fig. 21. J's effect on Temperature

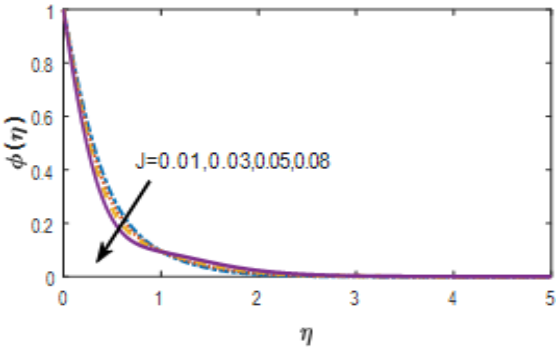

Fig. 22. J's effect on Concentration

In Figure 23, it has been observed that the number of Skin-friction coefficients rises as the Forchheimer parameter's value rises. Figure 24 and Figure 25 exhibit the Nusselt number for varying parameters Nb and Nt. It is noted that Nusselt number decreases with increment in Nb and Nt (with variation of Pr values). In Figure 26 and Figure 27, the Shear wood number is displayed for several parameters Nb and Nt. It is noted that the Shear wood number increases as Nb and Nt increase.

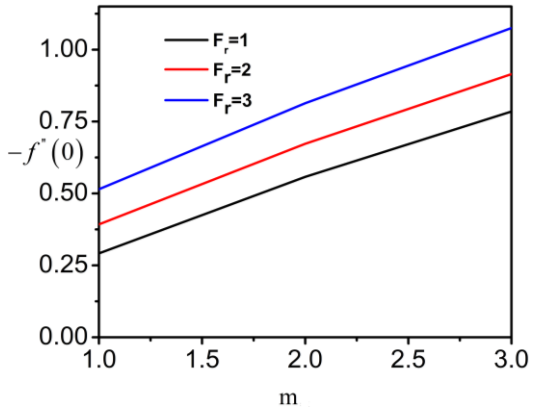

Fig. 23. m's and F_r 's effect on $-f''(0)$

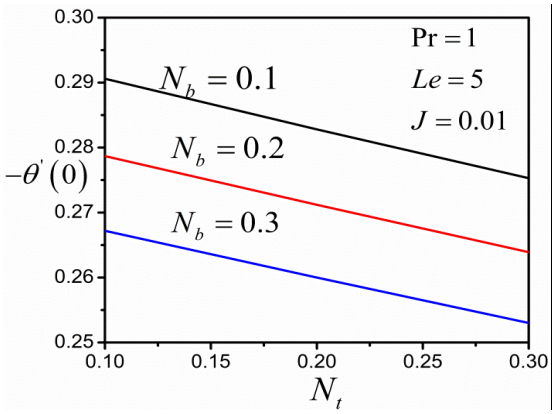

Fig. 24. Nt's and Nb's effect on $-\theta'(0)$

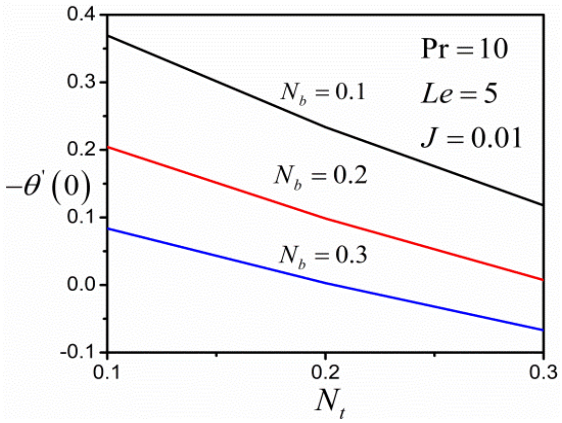

Fig. 25. Nt 's and Nb's effect on $-\theta'(0)$

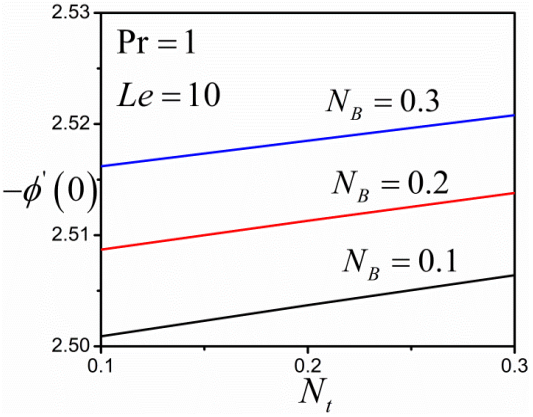

Fig. 26. Nt's and Nb's effect on $-\phi'(0)$

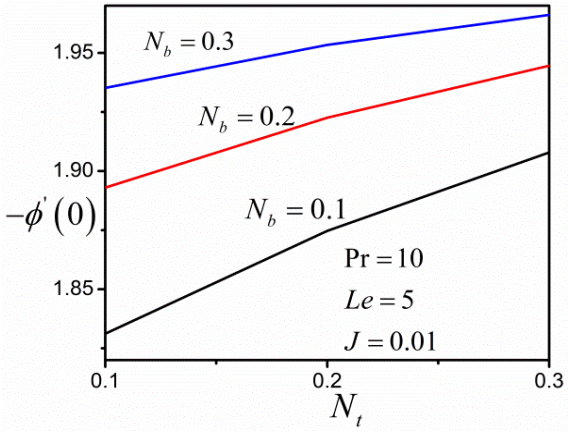

Fig. 27. Impact of Nt, Nb on $-\phi'(0)$ with different values of Pr, Le and J

Table 1 displays comparison of present results $-\theta'(0)$ and $-\phi'(0)$ with the previous and Table 2 demonstrates the impact of several non- dimensional parameters on the coefficient of skin friction, Nusselt number $-\phi'(0)$ and shear wood number $-\phi'(0)$.

Table 1
Comparison of the reduced $-\theta'(0)$ and $-\phi'(0)$ when $M, R, \delta, Sr, D_f, J, H, K_r, \lambda = 0, \beta \to \infty, m = 1$ *and*, $\Pr = Le = 10$ *and* $\gamma = 90^\circ$

N_b	N_t	$-\theta'(0)$			$-\phi'(0)$		
		Khan *et al.*, [10]	Rafique *et al.*, [33]	Present	Khan *et al.*, [10]	Rafique *et al.*, [33]	Present
0.1	0.1	0.9524	0.9524	0.9166	2.1294	2.1294	2.3954
0.2	0.2	0.3654	0.3654	0.3372	2.5152	2.5152	2.8052
0.3	0.3	0.1355	0.1356	0.1240	2.6088	2.6088	2.8955
0.4	0.4	0.0495	0.0495	0.0456	2.6088	2.6088	2.8955
0.5	0.5	0.0179	0.0179	0.0175	2.5731	2.5731	2.7815

Table 2

Values of the $-\theta'(0)$, $-\phi'(0)$ and Skin-friction coefficient $-f''(0)$

N_b	Nt	Pr	Le	R	β	λ	δ	Sr	D_f	m	γ	J	K_r	H	$-f''(0)$	$-\theta'(0)$	$-\phi'(0)$
0.1	0.1	6.5	5	1.0	1.0	0.1	0.9	0.1	0.1	0.1	45°	0.01	0.1	0.0	0.1103	0.4421	1.1779
0.5															0.1195	0.0986	1.8993
	0.5														0.1229	0.1532	1.8594
		10													0.1059	0.3694	1.8312
			10												0.1625	0.2147	2.7391
				5.0											0.1328	0.3795	1.7367
					5.0										0.0717	0.4526	1.7606
						0.5									0.2681	0.4438	1.7467
							2.0								0.0276	0.4408	1.7994
								0.2							0.0847	0.4264	1.8238
									0.2						0.1284	0.2006	2.0060
										1.0					0.0686	0.4407	1.7881
											60°				0.1607	0.4425	1.7703
												0.02			0.1193	0.1636	1.8732
													0.2		0.1119	0.4344	1.8090
														0.2	0.0215	0.4392	1.7979

5. Conclusions

The current study reports on the radiative Darcy-Forchheimer squeezed flow of an unstable magneto-hydrodynamic non-Newtonian Casson fluid over a stretching sheet with heat production or absorption and Joule heating in the presence of chemical reaction effects. The resulting partial differential equations are transformed to Ordinary differential equations solved numerically by Keller-Box method. The primary outcomes from the fluid flow properties, moment, temperature, and concentration are presented graphically and analysed.

i. An increasing in the Magnetic parameter leads to decline in velocity and rise in temperature.
ii. It is also observed that the temperature profile increase whereas concentration propile declines with the Joule heating parameter.
iii. The velocity profile drops while temperature increases with an increasing in the F_r number.
iv. With rising Prandtl number (Pr) values, the thermophores (Nt), Brownian motion (Nb), radiation (R), Joule parameter, and thermal boundary layer thickness enrich and decrease.
v. The Concentration profile increases with increasing values of Sorret (So) while it drops for Joule number.
vi. Skin friction coefficient is increases with increasing values of $m \text{ and } F_r$.
vii. Nusselt number decreases with increase in $Nt \text{ and } Nb$ for different values of Pr and J.

References

[1] Choi, S. U. S., and Jeffrey A. Eastman. *Enhancing thermal conductivity of fluids with nanoparticles*. No. ANL/MSD/CP-84938; CONF-951135-29. Argonne National Lab.(ANL), Argonne, IL (United States), 1995.
[2] Buongiorno, Jacopo. "Convective transport in nanofluids." *ASME Journal of Heat and Mass Transfer* 128, no. 3 (2006): 240-250. https://doi.org/10.1115/1.2150834
[3] Elbashbeshy, Elsayed M. A., and Hamada Galal Asker. "Fluid flow over a vertical stretching surface within a porous medium filled by a nanofluid containing gyrotactic microorganisms." *The European Physical Journal Plus* 137, no. 5 (2022): 541. https://doi.org/10.1140/epjp/s13360-022-02682-y
[4] Tawade, Jagadish V., C. N. Guled, Samad Noeiaghdam, Unai Fernandez-Gamiz, Vediyappan Govindan, and Sundarappan Balamuralitharan. "Effects of thermophoresis and Brownian motion for thermal and chemically reacting Casson nanofluid flow over a linearly stretching sheet." *Results in Engineering* 15 (2022): 100448. https://doi.org/10.1016/j.rineng.2022.100448
[5] Nath, Ratnadeep, and Krishnan Murugesan. "Impact of nanoparticle shape on thermo-solutal buoyancy induced lid-driven-cavity with inclined magnetic-field." *Propulsion and Power Research* 11, no. 1 (2022): 97-117. https://doi.org/10.1016/j.jppr.2022.01.002
[6] Ahmad, Sohail, Kashif Ali, Muhammad Rizwan, and Muhammad Ashraf. "Heat and mass transfer attributes of copper-aluminum oxide hybrid nanoparticles flow through a porous medium." *Case Studies in Thermal Engineering* 25 (2021): 100932. https://doi.org/10.1016/j.csite.2021.100932
[7] Ziaei-Rad, Masoud, Abbas Kasaeipoor, Mohammad Mehdi Rashidi, and Giulio Lorenzini. "A similarity solution for mixed-convection boundary layer nanofluid flow on an inclined permeable surface." *Journal of Thermal Science and Engineering Applications* 9, no. 2 (2017): 021015. https://doi.org/10.1115/1.4035733
[8] Thumma, Thirupathi, O. Anwar Bég, and Siva Reddy Sheri. "Finite element computation of magnetohydrodynamic nanofluid convection from an oscillating inclined plate with radiative flux, heat source and variable temperature effects." *Proceedings of the Institution of Mechanical Engineers, Part N: Journal of Nanomaterials, Nanoengineering and Nanosystems* 231, no. 4 (2017): 179-194. https://doi.org/10.1177/2397791417731452
[9] Selva Rani, M., and A. Govindarajan. "Radiative fluid flow of a nanofluid over an inclined plate with non-uniform surface temperature." In *Journal of Physics: Conference Series*, vol. 1000, p. 012173. IOP Publishing, 2018. https://doi.org/10.1088/1742-6596/1000/1/012173
[10] Khan, Mair, Amna Shahid, M. Y. Malik, and T. Salahuddin. "Thermal and concentration diffusion in Jeffery nanofluid flow over an inclined stretching sheet: A generalized Fourier's and Fick's perspective." *Journal of Molecular Liquids* 251 (2018): 7-14. https://doi.org/10.1016/j.molliq.2017.12.001

[11] Sarkar, Amit, and Prabir Kumar Kundu. "Darcy-Forchheimer flow of Cu-water nanofluid over a vertical sheet owing to solar radiation." *Pramana* 95, no. 4 (2021): 177. https://doi.org/10.1007/s12043-021-02214-w
[12] Bhatti, Muhammad Mubashir, S. R. Mishra, Tehseen Abbas, and Mohammad Mehdi Rashidi. "A mathematical model of MHD nanofluid flow having gyrotactic microorganisms with thermal radiation and chemical reaction effects." *Neural Computing and Applications* 30 (2018): 1237-1249. https://doi.org/10.1007/s00521-016-2768-8
[13] Sakiadis, Byron C. "Boundary-layer behavior on continuous solid surfaces: I. Boundary-layer equations for two-dimensional and axisymmetric flow." *AIChE Journal* 7, no. 1 (1961): 26-28. https://doi.org/10.1002/aic.690070108
[14] Konwar, Hemanta, Bendangwapang, and Temjennaro Jamir. "Mixed convection MHD boundary layer flow, heat, and mass transfer past an exponential stretching sheet in porous medium with temperature-dependent fluid properties." *Numerical Heat Transfer, Part A: Applications* 83, no. 12 (2023): 1346-1364. https://doi.org/10.1080/10407782.2022.2104581
[15] Ali, Mohammad, Md Abdul Alim, and Mohammad Shah Alam. "Heat transfer boundary layer flow past an inclined stretching sheet in the presence of magnetic field." *International Journal of Advancements in Research & Technology* 3, no. 5 (2014): 34-40.
[16] Ramesh, G. K., B. J. Gireesha, and C. S. Bagewadi. "Heat transfer in MHD dusty boundary layer flow over an inclined stretching sheet with non-uniform heat source/sink." *Advances in Mathematical Physics* 2012 (2012). https://doi.org/10.1155/2012/657805
[17] Malik, M. Y., and Khalil Ur Rehman. "Effects of second order chemical reaction on MHD free convection dissipative fluid flow past an inclined porous surface by way of heat generation: A Lie group analysis." *Information Sciences Letters* 5, no. 2 (2016): 35-45. https://doi.org/10.18576/isl/050201
[18] Ramesh, G. K., A. J. Chamkha, and B. J. Gireesha. "Boundary layer flow past an inclined stationary/moving flat plate with convective boundary condition." *Afrika Matematika* 27 (2016): 87-95. https://doi.org/10.1007/s13370-015-0323-x
[19] Griffiths, Paul T. "Stability of the shear-thinning boundary-layer flow over a flat inclined plate." *Proceedings of the Royal Society A: Mathematical, Physical and Engineering Sciences* 473, no. 2205 (2017): 20170350. https://doi.org/10.1098/rspa.2017.0350
[20] Pal, Dulal, and Hiranmoy Mondal. "Influence of Soret-Dufour and thermophoresis on hydromagnetic mixed convection heat and mass transfer over an inclined flat plate with non-uniform heat source/sink and chemical reaction." *International Journal for Computational Methods in Engineering Science and Mechanics* 19, no. 2 (2018): 49-60. https://doi.org/10.1080/15502287.2018.1430073
[21] Pandya, N., and A. K. Shukla. "Soret-Dufour and radiation effect on unsteady MHD flow over an inclined porous plate embedded in porous medium with viscous dissipation." *International Journal of Advances in Applied Mathematics and Mechanics* 2, no. 1 (2014): 107-119.
[22] Bhatti, Muhammad Mubashir, Munawwar Ali Abbas, and Mohammad Mehdi Rashidi. "Entropy generation for peristaltic blood flow with casson model and consideration of magnetohydrodynamics effects." *Walailak Journal of Science and Technology (WJST)* 14, no. 6 (2017): 451-461.
[23] Yanala, Dharmendar Reddy, M. Anil Kumar, Shankar Goud Bejawada, Kottakkaran Sooppy Nisar, R. Srinivasa Raju, and V. Srinivasa Rao. "Exploration of heat and mass transfer on 3-D radiative MHD Casson fluid flow over a stretching permeable sheet with chemical reaction." *Case Studies in Thermal Engineering* 51 (2023): 103527. https://doi.org/10.1016/j.csite.2023.103527
[24] Shamshuddin, M. D., S. R. Mishra, and Thirupathi Thumma. "Chemically reacting radiative Casson fluid over an inclined porous plate: a numerical study." In *Numerical Heat Transfer and Fluid Flow: Select Proceedings of NHTFF 2018*, pp. 469-479. Singapore: Springer Singapore, 2018. https://doi.org/10.1007/978-981-13-1903-7_54
[25] Prasad, D. V. V., G. S. Chaitanya, and R. Srinivasa Raju. "Role of casson fluid on MHD natural convective flow towards vertically inclined plate with hall current." In *AIP Conference Proceedings*, vol. 1953, no. 1. AIP Publishing, 2018. https://doi.org/10.1063/1.5033248
[26] Jain, Shalini, and Amit Parmar. "Multiple slip effects on inclined MHD Casson fluid flow over a permeable stretching surface and a melting surface." *International Journal of Heat and Technology* 36, no. 2 (2018): 585-594. https://doi.org/10.18280/ijht.360222
[27] Babu, D. Harish, and PV Satya Narayana. "Joule heating effects on MHD mixed convection of a Jeffrey fluid over a stretching sheet with power law heat flux: A numerical study." *Journal of Magnetism and Magnetic Materials* 412 (2016): 185-193. https://doi.org/10.1016/j.jmmm.2016.04.011
[28] Rao, Jakkula Anand, Gandamalla Vasumathi, and Jakkula Mounica. "Joule heating and thermal radiation effects on MHD boundary layer flow of a nanofluid over an exponentially stretching sheet in a porous medium." *World Journal of Mechanics* 5, no. 09 (2015): 151-164. https://doi.org/10.4236/wjm.2015.59016

[29] Ur Rasheed, Haroon, Abdou AL-Zubaidi, Saeed Islam, Salman Saleem, Zeeshan Khan, and Waris Khan. "Effects of Joule heating and viscous dissipation on magnetohydrodynamic boundary layer flow of Jeffrey nanofluid over a vertically stretching cylinder." *Coatings* 11, no. 3 (2021): 353. https://doi.org/10.3390/coatings11030353

[30] Mao, J., Svetlana Aleksandrova, and Sergei Molokov. "Joule heating in magnetohydrodynamic flows in channels with thin conducting walls." *International Journal of Heat and Mass Transfer* 51, no. 17-18 (2008): 4392-4399. https://doi.org/10.1016/j.ijheatmasstransfer.2008.02.005

[31] Ganesh, N. Vishnu, AK Abdul Hakeem, and B. Ganga. "Darcy-Forchheimer flow of hydromagnetic nanofluid over a stretching/shrinking sheet in a thermally stratified porous medium with second order slip, viscous and Ohmic dissipations effects." *Ain Shams Engineering Journal* 9, no. 4 (2018): 939-951. https://doi.org/10.1016/j.asej.2016.04.019

[32] Haider, Farwa, Tasawar Hayat, and Ahmed Alsaedi. "Flow of hybrid nanofluid through Darcy-Forchheimer porous space with variable characteristics." *Alexandria Engineering Journal* 60, no. 3 (2021): 3047-3056. https://doi.org/10.1016/j.aej.2021.01.021

[33] Rafique, Khuram, Muhammad Imran Anwar, Masnita Misiran, Ilyas Khan, S. O. Alharbi, Phatiphat Thounthong, and K. S. Nisar. "Numerical solution of casson nanofluid flow over a non-linear inclined surface with soret and dufour effects by keller-box method." *Frontiers in Physics* 7 (2019): 139. https://doi.org/10.3389/fphy.2019.00139